Deep-Sea Research Part I 141 (2018) 118–129

Contents lists available at ScienceDirect

Deep-Sea Research Part I

journal homepage: www.elsevier.com/locate/dsri

Phytoplankton response in growth, photophysiology and community structure to iron and light in the Polar Frontal Zone and Antarctic waters

Johannes J. Viljoen[a,1], Raïssa Philibert[a,1,2], Natasha Van Horsten[a,b], Thato Mtshali[b], Alakendra N. Roychoudhury[a], Sandy Thomalla[b], Susanne Fietz[a,*]

[a] Department of Earth Sciences, Stellenbosch University, 7600 Stellenbosch, South Africa
[b] Southern Ocean Carbon and Climate Observatory, CSIR, 7599 Stellenbosch, South Africa

ARTICLE INFO

Keywords:
Bioassay
GEOTRACES
Iron fertilization
Pigments
CHEMTAX

ABSTRACT

Availability of dissolved iron and light are both regulating factors for primary productivity in high (macro) nutrient, low chlorophyll regions of the Southern Ocean. Here, using on-board iron/light incubation experiments conducted in 2015 in the Atlantic sector of the Southern Ocean, we show that irradiance limited significant phytoplankton growth (in chlorophyll-a and particulate organic carbon) north of the Polar Front (46 °S 08 °E), while iron addition resulted in growth stimulation even at low light levels in the Antarctic zone (65 °S 0 °E). The phytoplankton community in the Polar Frontal Zone showed a greater functional diversity than the one in the Antarctic Zone. The community structure changed over the course of the incubations in response to increased iron and light. The observed increase in chlorophyll-a under high light in the Polar Frontal Zone was driven predominantly by an increase in pico-(0.2–2 µm) and large (> 5 µm) nanophytoplankton. Pigment fingerprinting indicated an increase in the contribution of diatoms and Phaeocystis over the course of the incubation. In contrast, in the Antarctic Zone, the increase in chlorophyll-a after iron enrichment was predominantly due to an increase in the contribution of diatoms and large nanophytoplankton. The photochemical efficiency (Fv/Fm) was low at both sites at the beginning of the incubations, but increased upon iron fertilization in both water masses, indicating stress relief. However, the acclimation strategies fundamentally differed between the two communities. The ratio of photoprotective versus light-harvesting pigments increased under high light in the Polar Frontal Zone independent of iron enrichment, whereas this ratio declined upon iron enrichment in the Antarctic Zone even under high light. At the same time, the functional cross section of photosystem II (σ_{PSII}) decreased upon iron enrichment in the Antarctic Zone, but not in the Polar Frontal Zone. Our experiments support the need to take biogeographical differences between Southern Ocean water masses into account when interpreting ecosystem dynamics.

1. Introduction

The ocean plays a crucial role in controlling the concentration of atmospheric CO_2 and consequently the Earth's climate. The Southern Ocean in particular accounts for ~33% of the global organic carbon flux (Schlitzer, 2002), which is largely driven by phytoplankton growth and the subsequent sinking and sequestration of organic matter. Given phytoplankton's role in carbon cycling and its associated impact on climate, it is important that we understand the factors regulating their growth, photosynthetic performance and community structure.

It is well-established that phytoplankton growth in the Southern Ocean is limited by iron and light availability (Boyd et al., 2010; de Baar et al., 1990; Martin et al., 1990), which leads to the occurrence of High (macro)Nutrients, Low Chlorophyll (HNLC) regions. Iron is a vital micronutrient for phytoplankton functionality, especially in photosynthesis because of its requirement in photosynthetic electron transport (e.g. PSI, PSII, the Cytochrome b_6-f-FeS complex; Raven, 1990; Strzepek and Harrison, 2004). Subnanomolar iron concentrations are observed in HNLC regions due to limited external or continental iron inputs (e.g., from dust, rivers and shelf sediments), low solubility,

Abbreviations: AAZ, Antarctic Zone of the Southern Ocean; PFZ, Polar Frontal Zone of the Southern Ocean

* Corresponding author.
E-mail address: sfietz@sun.ac.za (S. Fietz).

[1] These authors contributed equally.
[2] Current address: Hatfield Consultants, North Vancouver, BC, Canada.

https://doi.org/10.1016/j.dsr.2018.09.006
Received 7 May 2018; Received in revised form 31 August 2018; Accepted 17 September 2018
Available online 19 September 2018
0967-0637/

internal recycling and/or access to deep iron rich reservoirs (Boyd and Ellwood, 2010). Where there are no other limiting factors, sudden iron addition leads to enhanced phytoplankton growth in the Southern Ocean and artificial fertilization experiments conducted over the past two decades have unequivocally led to phytoplankton blooms in iron limited regions (e.g., Boyd et al., 2000; Coale et al., 2004; Lance et al., 2007; Moore et al., 2013).

However, phytoplankton growth is often limited by more than one factor (Moore et al., 2013). Limitation in the natural environment might happen in different ways, either one factor represents the primary limiting factor, e.g. iron, with the other one, e.g. light, being the next limiting factor if iron is relieved, or both are required simultaneously (Saito et al., 2008). In studies using in-situ assemblage or single phytoplankton species, artificial iron enrichment led not only to growth stimulation, but also to enhanced photochemical efficiency and structural changes in the photosystems (Petrou et al., 2014; Strzepek et al., 2012) due to the involvement of iron in major photosynthetic processes (Behrenfeld and Milligan, 2013; Morel et al., 2003). The strong coupling between iron availability and photosynthetic physiology suggests that dependent co-limitation (Saito et al., 2008) between iron and light availability is likely to occur, where iron for example can only be utilized under sufficient light availability, or vice versa. This means that iron and light limitation can exacerbate each other (Sunda, 1997). However, culture studies have also demonstrated that the phytoplankton response to iron and light limitation can be group and/or species specific and that some Southern Ocean phytoplankton are able to thrive under low iron and low light conditions (DiTullio et al., 2007; Timmermans et al., 2005, 2001). This could mean that the response of Southern Ocean phytoplankton to changes in iron and light conditions may occur at community level, instead of or in addition to cellular acclimation. Therefore, although uni-algal cultures can provide insights into the mechanisms controlling iron and light limitation, experiments with whole phytoplankton communities are desirable as they highlight changes at the community level.

Physical properties (e.g., temperature, salinity, light intensity, mixing regime, day length; Carter et al., 2008) and chemical properties (e.g., nitrate, silicate, iron availability; Klunder et al., 2011; Pollard et al., 2002) vary across oceanic regions. Furthermore, changes due to projected climate change are also likely to vary considerably across oceanic regions (e.g., Deppeler and Davidson, 2017; Howes et al., 2015). As a consequence, responses of phytoplankton communities to changes in light and iron are unlikely to be uniform across varying water masses. Experiments on in-situ communities have investigated iron and light co-regulation for phytoplankton growth in the South Indian Ocean (Cheah et al., 2013; Moore et al., 2007), south of Tasmania (Cheah et al., 2013; Petrou et al., 2011), in the South Pacific Ocean (Peloquin et al., 2011), the Ross Sea (Feng et al., 2010) and in other Antarctic regions (Alderkamp et al., 2012; Mills et al., 2012), where the natural iron supply is temporarily enhanced due to land runoff or ice melt. However, there are very few studies in the open Atlantic Southern Ocean on iron and light co-regulation. van Oijen et al. (2004) established that in autumn, phytoplankton in the Atlantic Southern Ocean was light rather than iron limited, while Boyd and Abraham (2001), in the Pacific Southern Ocean, observed iron limitation north of the Subantarctic Front at 47 °S but iron and light co-limitation south of the Subantarctic Front at 54 °S.

Here we expand on these studies by comparing the response of bulk communities to iron enrichment and exposure to higher light in the Atlantic Southern Ocean, at two stations; one north of the Polar Front at 46 °S and the other in Antarctic Waters at 65 °S, with a focus on changes in growth, community structure and photophysiology. We evaluate changes in the phytoplankton community composition using marker pigments and the CHEMTAX matrix factorisation programme (Mackey et al., 1996; Wright et al., 2010), along with size fractionated chl-a measurements. To further investigate the photophysiological response to iron and light enrichment we use photosynthetic efficiency (Fv/Fm), and the absorption cross-section of photosystem II (σ_{PSII}) as well as changes in photoprotective pigments. We aim to test whether the Southern Ocean community response in growth, structure and physiology is regulated by dependent co-limitation of iron and light. We hypothesise that the type of response to iron or light is regionally different in the Southern Ocean. With this we aim to improve our understanding of the consequences of key environmental changes in the present and future ocean.

2. Methods

2.1. Sampling stations

The iron and light incubation experiments were conducted during the 54th South African National Antarctic Expedition (SANAE) from December 2014 to February 2015 (from here on referred to as S54). The cruise track mainly followed the Good Hope monitoring line (Fig. 1) crossing the Subtropical Front, Subantarctic Front and Polar Front until the Antarctic ice shelf was reached. The Good Hope line generally crosses the Subantarctic Front and Polar Front at about 45 °S and 49 °S, respectively, with some seasonal and interannual variability (Billany et al., 2010). The frontal positions at the time of this study were identified based on temperature data from the eXpendable BathyThermographs (XBT) transects AX25 (NOAA, 2015). During S54, the south-bound AX25 transect from December 2014 was used. The frontal detection criteria set by Orsi et al. (1995), from 4 to 5 °C at 400 m for the Subantarctic Front and 2 °C at 200 m for the Polar Front, were used. Following this approach, during S54, the Subtropical Front was situated at 40.4 °S, the Subantarctic Front at 44.1 °S and the Polar Front at 50.4 °S (Fig. 1). Two stations were visited during this mid-summer cruise: S54-46 (46.00 °S 08.00 °E) within the Polar Frontal Zone (PFZ) and S54–65 (65.00°S 00.00 °E) within the Antarctic zone (AAZ; Fig. 1).

2.2. Sampling and incubation set-up

At both stations, temperature (Supplemental information Fig. S1) and salinity profiles were obtained from a Sea-Bird CTD (Sea-Bird Electronics, USA) mounted on the CTD rosette. The mixed layer depth (Table 1) was identified from the temperature profiles as the first depth where the temperature differs from the temperature at 10 m by more than 0.2 °C (de Boyer Montégut et al., 2004). A fluorescence sensor was also attached to the rosette. The fluorescence signal (Fig. S1) was corrected for quenching and calibrated against bottle measurements of chl-a. Seawater for incubation experiments was collected from the apparent depths of fluorescence maxima at the bottom of the mixed layer at both stations (ca. 85 m at 46 °S, station S54-46, and ca. 30 m at 65 °S, station S54–65; Fig. S1). The seawater was sampled according to GEOTRACES trace metal clean protocols (Cutter et al., 2014; Cutter and Bruland, 2012) using an epoxy coated aluminium frame CTD rosette equipped with 24 × 12-L GoFlo sampling bottles. Sample preparation and manipulation were conducted inside a class 100 trace metal clean container. The seawater was filtered through a 200 µm pore size mesh into two acid-washed (details provided in Supplemental information) 50-L low-density polyethylene (LDPE) carboys (Thermo Fisher Scientific, USA). The homogenised seawater was then redistributed equally into acid washed 2.4-L Nalgene™ polycarbonate bottles (Thermo Fisher Scientific, USA; Supplemental information Fig. S2).

To characterise initial conditions three sample bottles were analysed immediately (details follow below). Further 36 bottles were incubated under four different iron/light treatments (details follow below) in specifically designed incubators (Minus40 Specialised Refrigeration, South Africa). The incubators were equipped with adjustable light-emitting diode (LED) strips above each shelf and a cooling fan for temperature control. Temperatures were set to mimic the respective in-situ temperatures (Table 1) for both experiments using the incubators' built-in temperature control systems, which maintained the

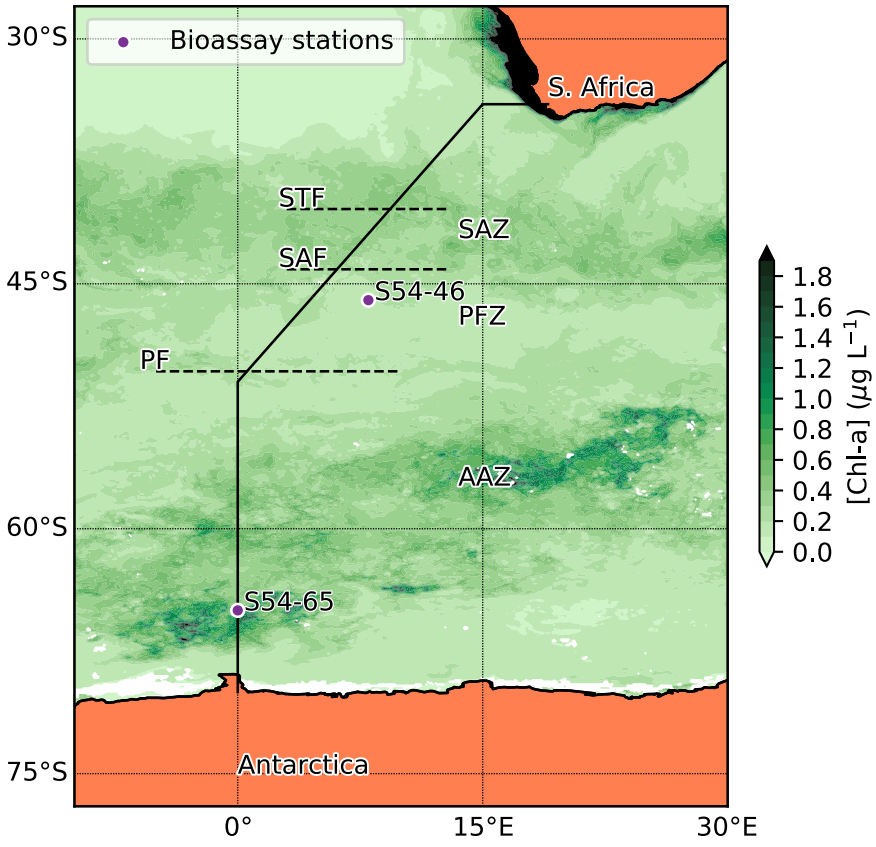

Fig. 1. Station positions along the Good Hope line for cruise SANAE54. The background shows a seasonal composite of chl-a concentration for the period of December 2014 to February 2015 (NASA Ocean Biology Processing Group, 2014). The solid black line represents the Good Hope line. The dashed horizontal lines indicate the frontal positions (STF - subtropical front, SAF - Subantarctic Front, PF - Polar Front) along the Good Hope line. Black regions on the map represent areas where the chl-a concentration is higher than 2 μg L^{-1} whereas white regions indicate insufficient chl-a data due to ice or cloud cover.

temperature within a range of ± 0.5 °C. Temperatures were monitored using a handheld thermometer probe (Penta Digital, USA). Light levels were set using a handheld 4π photosynthetically active radiation (PAR) sensor (Biosphere QSL 2100, Biospherical Instruments Inc., USA). Day:night cycles were adjusted according to in-situ day:night cycles at the time and site of sampling (Supplemental Information).

Briefly, treatments consisted of i) low light level, no iron addition (L1), ii) low light level and iron addition (L1 + Fe), iii) higher light intensities, no iron addition (L2), and iv) higher light intensities and iron addition (L2 + Fe). Each treatment was conducted in triplicate bottles (Fig. S2). The low light level (L1) was set to the in-situ PAR (15 μE m^{-2} s^{-1}; Fig. S1) measured at the time (early afternoon) and depth (chl-a maximum; ca. 85 m) of sampling for the station at 46 °S. For the station at 65 °S, the measured in-situ PAR at the sampling depth (chl-a maximum; ca. 30 m) and time (early morning) was 0 μE m^{-2} s^{-1} (Fig. S1), which represents an unsuitable light level for incubation studies. Therefore, low light level (L1) was set to PAR at 10 m depth (25 μE m^{-2} s^{-1}; Fig. S1). The high light (L2) was set to 65 μE m^{-2} s^{-1} for both sites. Synthetic iron was added as 1 nM $FeCl_3$ to the +Fe treatments under the laminar flow hood inside the onboard class 100 trace metal clean laboratory using an 89.5 μM acidic $FeCl_3$ solution made from a 1000 mg L^{-1} stock solution (Iron Atomic Spectroscopy Standard, Sigma Aldrich). Additions of 1 nM dissolved iron (dFe) have previously been shown to noticeably alleviate iron limitation (Boyd and Abraham, 2001) and were therefore considered to be appropriate for this set of experiments. Further details of the incubations are given in the Supplemental Information.

The dFe of the initial seawater was analysed in triplicate for both incubation experiments (S54-45 and S54–65; Table 1). Sample processing and analysis for dFe followed GEOTRACES guidelines (Cutter et al., 2014; Cutter and Bruland, 2012) inside the on-board class 100 clean container. The collected seawater was filtered for dFe determination from the GoFlo bottles into acid-washed 125 mL LDPE bottles through 0.2 μm pore size Acropak™ 500 Supor® membrane filters with filtered (Midisart 2000, 0.20 μm) nitrogen assistance (BIP Technology). All samples were immediately acidified using hydrochloric acid (Ultrapur, Merck) to a pH of 1.7 and stored. A SeaFAST-pico SC-4 DX (Elemental Scientific) module was used for offline pre-concentration (by a factor of 40 times) inside a class 100 trace metal clean laboratory, prior to injection into a quadrupole inductively coupled plasma mass spectrometer (ICP-MS; Agilent 7900) at Stellenbosch University, South Africa. Details on the acid-washing of material, the instrument configuration and chelating resin as well as intercalibration, within laboratory calibration and check standards are provided by Cloete et al. (revisions submitted). Depth profiles for the dissolved bioactive trace metals Cu, Zn, Cd, Co, and Mn for stations along the SANAE 54 transect including

Table 1
Site characteristics and initial conditions for both incubation experiments. The temperature and salinity were extracted from the CTD sensor data for both stations. The initial nutrient concentrations (NO_3^- and $Si(OH)_4$) were obtained from discrete samples taken on a separate cast at the same station. The mixed layer depth (MLD) was calculated according to the temperature criteria by de de Boyer Montégut et al. (2004). Example profiles of temperature, light attenuation and chl-a concentrations at both stations are shown in Supplemental Fig. S1.

	S54-46	S54–65
Date	12-Jan-15	18-Jan-15
Latitude (°S)	46	65
Longitude (°E)	8	0
Region	PFZ	AAZ
Temperature (°C)	6.20	0.00
Salinity	33.8	34.0
MLD (m)	89	31
[dFe] (nM)	0.37	0.19
[NO^-_3] (μM)	23.3	25.2
[$Si(OH)_4$] (μM)	5.79	74.3

S54-46 and S54–65 are presented in Cloete et al. (revisions submitted) and Loock et al. (in revision).

2.3. Measurements of growth and photophysiology

Concentrations of total chl-a, particulate organic carbon (POC) and dissolved nutrients (NO_3^- + NO_2^-, PO_4^{3-} and $Si(OH)_4$) were measured to determine differences in growth and nutrient uptake between treatments. Samples for frequent (ca 48 h) determination of total chl-a were filtered through glass fibre filters with nominal pore sizes of 0.2, 2 and 5 µm, frozen for 24 h, extracted in 90% acetone and analysed using a Turner fluorometer. Chl-a concentrations for pico- (0.2–2 µm), nano- (2–5 µm) and micro-phytoplankton (> 5 µm) were measured to obtain information on the size structure of the phytoplankton community. Samples for POC were filtered through ashed glass fibre filters with a nominal pore size of 0.7 µm. The filters were acid fumed to remove any inorganic carbon and analysed using an elemental analyser. Nutrient concentrations were determined using a flow injection autoanalyser for NO_3^- + NO_2^- and $Si(OH)_4$ (Egan, 2008; Wolters, 2002), while PO_4^{3-} concentrations were determined manually according to the methods described by Grasshoff et al. (1983). Incubation bottles were sampled for all variables at four time-points, i.e., at the start and end of the incubation and at two intermediary time points. Photophysiology analysis (Fv/Fm and σ_{PSII}) was conducted every 24 h using Fast Repetition Rate fluorometry (FRRf; Chelsea SMD Telecommunications (Pty) LTD, UK). Details on filters, instruments and calibration standards for chl-a, POC and macronutrients as well as on FRRf settings are provided in the Supplemental information. All statistical analyses were performed in R Statistical Software (R Core Team, 2015) and all graphs plotted with Ggplot2 (Wickham, 2009).

2.4. Determination of accessory pigments and community composition

Samples were also taken for accessory pigment analysis. Amber sample bottles were used for subsampling from the incubation bottles and filtration carried out under dim light due to the sensitivity of accessory pigments to light. The water was filtered through glass fibre filters (0.7 µm nominal pore size) and filters immediately stored at − 80 °C until analysis. Analysis for phytoplankton pigments by High-Performance Liquid Chromatography (HPLC) was conducted at Laboratoire d'Océanographie de Villefranche-sur-Mer as described by Ras et al. (2008). Phytoplankton pigment samples were collected only at the start of the experiment and again at the final termination after five to six days of incubation to represent the community for the initial conditions and at the end of each treatment. Detailed pigment data are provided in Table S1. In this study we will focus on phytoplankton chemotaxonomic composition and specific pigment ratios indicative for photoacclimation.

The contribution of individual phytoplankton functional groups to total chl-a (used here as a proxy for biomass) was calculated using the CHEMTAX v1.95 chemical taxonomy software (Mackey et al., 1996; Wright et al., 2010). The CHEMTAX phytoplankton community composition estimates are based on the relative abundance of a suite of marker pigments to total chl-a in the water. Each group has a characteristic pool of accessory pigments, but all phytoplankton groups contribute to the total chl-a. However, the interpretation of pigment data for the assessment of community composition can be difficult due to marker pigments that are present in several groups. The CHEMTAX matrix factorisation is therefore based on the ratios between one or more accessory pigments and chl-a per group (Mackey et al., 1996; Wright et al., 2010). Below we briefly describe the approach of the CHEMTAX protocol for the identification of phytoplankton functional groups and determination of their relative abundances.

The main phytoplankton groups to be included into the CHEMTAX processing were selected based on literature data published for the Atlantic Southern Ocean and nearby regions (Gibberd et al., 2013; Mendes et al., 2015; Schlüter et al., 2011; Wright et al., 2010). Nine phytoplankton chemotaxonomic groups were chosen (cryptophytes were excluded from the CHEMTAX calculations, since alloxanthin, their marker pigment, was not detected): cyanobacteria, prasinophytes, pelagophytes (Pelagophyte pigment Type 1; Mendes et al., 2015; Schlüter et al., 2011), chlorophytes, dinoflagellates, diatoms, and three groups of haptophytes, i.e. coccolithophores (Haptophyte pigment Type 6; Zapata et al., 2004), Phaeocystis-H (Haptophyte pigment Type 8, in the Southern Ocean represented by *Phaeocystis antarctica,* acclimated to high iron availability), and Phaeocystis-L (*P. antarctica* acclimated to low iron availability; Wright et al., 2010). These two functional forms were included because *P. antarctica* adjust the pigment ratios to the ambient iron concentrations as observed in cultures grown under iron enriched vs. iron depleted conditions (DiTullio et al., 2007; Wright et al., 2010). Further details regarding the choice of specific pigments and phytoplankton groups for the CHEMTAX processing as well as the optimised ratios after the CHEMTAX analyses can be found in the Supplemental Information and Table S2. As outlined above (2.2 Sampling and incubation set-up), each experiment was conducted in triplicate and hence estimates of contributions of phytoplankton groups were obtained in triplicate. These triplicate contributions were averaged (Table S3) similarly to all other parameters presented in this study for each treatment.

3. Results

3.1. Sampling site characterisation

The observed in-situ conditions at both sites, at 46 °S (PFZ) and at 65 °S (AAZ) were characteristic of typical conditions of the respective water masses. Average surface temperatures between January and March generally range between 6 and 9 °C for PFZ and below 5 °C for the AAZ (Boyer et al., 2013). Average January to March nitrate concentrations typically increase southwards from about 10 µM in the SAZ to 20 µM in the PFZ and > 25 µM in the AAZ (Boyer et al., 2013). Typical surface silicic acid concentrations are generally low throughout the Subantarctic Zone and PFZ (< 10 µM) and increase sharply south of the Polar Front to > 50 µM (Boyer et al., 2013). Table 1 summarises the in-situ conditions for our experiments. The station at 46 °S, was characterised by a deep mixed layer (89 m). Low temperatures (~ 6 °C) and low chl-a concentrations (0.12 µg L^{-1}) were observed at the sampling depth (depth of chlorophyll maximum). The nitrate concentration at 46 °S was relatively high (23 µM), while silicic acid concentrations were low (5.8 µM). Conditions at 65 °S in the AAZ were characterised by much lower temperatures (0 °C), relatively shallow mixed layer depths (31 m), and high chl-a (1 µg L^{-1}), nitrate (25 µM), and silicic acid (74 µM) concentrations. The molar $Si:NO_3$ ratio was ca. ten times higher in the AAZ (2.9) compared to the PFZ (0.25). The dFe concentrations were 0.37 nM at 46 °S and 0.19 nM at 65 °S (Table 1). The molar $dFe:NO_3$ ratios were thus 0.016×10^{-3} at 46 °S and 0.0075×10^{-3} at 65 °S.

The photosynthetic efficiency (Fv/Fm) and functional absorption cross-section of photosystem II (σ_{PSII}) further provide an indication of the nutrient limitation in phytoplankton. Under nutrient limitation, the photosynthetic efficiency (Fv/Fm) decreases. Such nutrient limitation can also cause a loss of reaction centres (where photochemical reactions leading to the evolution of O_2 occur) and may lead to an increase in the light absorption cross section (or light absorption coefficient) of PSII (σ_{PSII}; Suggett et al., 2004). The initial Fv/Fm values were around 0.25 at both stations (46 °S and 65 °S) indicating that the phytoplankton experienced stress and potential iron limitation prior to the incubation (Figs. 2a, 2c). The initial functional cross section of photosystem II (σ_{PSII}) was much higher at 65 °S compared to 46 °S (Fig. 2b, d).

In addition to the abiotic and physiological differences, the water masses studied here showed differences in the initial phytoplankton composition. At 46 °S, the largest cell fraction (> 5 µm) dominated

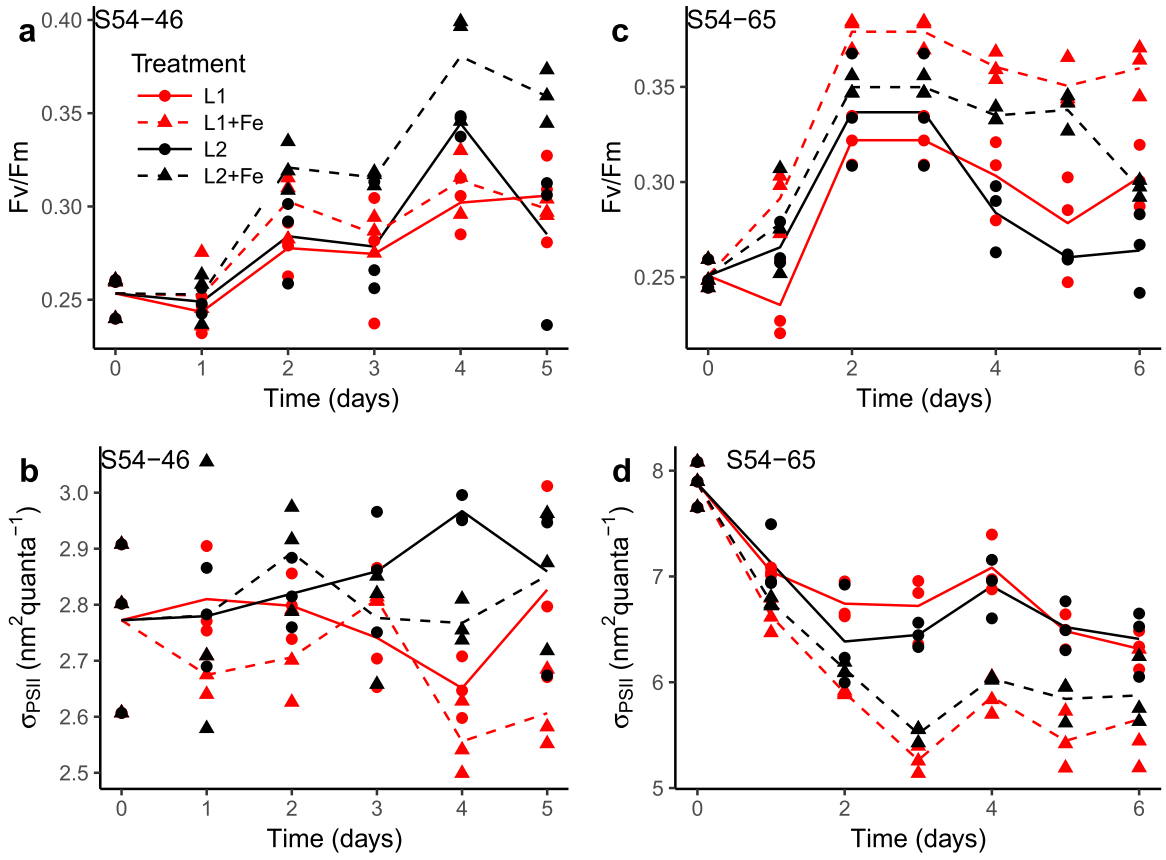

Fig. 2. Changes in Fv/Fm (a,c) and $\sigma_{PS\ II}$ (b,d) over the course of the two summer 2015 bioassays, S54-46 in the PFZ (a,b), and S54–65 in the AAZ (c,d). The red lines indicate the low light treatments (L1) and the black lines the higher light treatments (L2). Dashed lines and triangles are for iron enriched treatments (+Fe) while solid lines and circles indicate control conditions without iron enrichment. The symbols represent individual measurements at each time point (termination). The lines represent the average values of Fv/Fm and σ_{PSII} for each treatment. The y-axes for σ_{PSII} are shown on different scales due to the large differences between the two experiments. Statistically significant changes between Tf and T0 are only observed for the treatment L2 + Fe at station S54-46 and for treatment L1 + Fe at station S54–65. See Table S8 for statistical outcome of the Tf versus T0 comparison. For interpretation of the references to colour in the figure caption, the reader is referred to the online version of this article.

with a 48% contribution to total chl-a (Fig. 3a). The lowest chl-a contribution (14%) was observed in the 2–5 μm size fraction. The smallest size fraction (0.2–2 μm) contributed 38%. Pigment signatures indicated that the initial community in the PFZ was dominated by both Phaeocystis and diatoms with contributions of 45% and 43%, respectively and minor amounts of coccolithophores (Fig. 4a). This initial PFZ community also contained noticeable pico-phytoplankton contributions of prasinophytes (9%). In the AAZ, the largest cell fraction (> 5 μm) in the initial seawater dominated with 71% (Fig. 3b). Much lower chl-a contributions were observed in the 2–5 μm (16%) and 0.2–2 μm (13%) size fractions. The pigment composition suggests that those large cells were presumably diatoms and coccolithophores. Diatoms showed the largest contribution (62%) to chl-a in the AAZ, while haptophytes, including pigment category Haptophytes 6 (coccolithophores) and pigment category Haptophytes 8 (Phaeocystis; Zapata et al., 2004) contributed around 40% (Fig. 4b).

3.2. Responses to increasing iron and light in the PFZ (46 °S)

3.2.1. Indicators of stress relief

All treatments in the PFZ showed an increase in Fv/Fm over the course of the incubation (Fig. 2a). However, iron addition led to stronger initial increase in Fv/Fm compared to the non-amended treatments (Fig. 2a). The response in photochemical efficiency was rather quick: the L1 + Fe and L2 + Fe treatments showed higher Fv/Fm values than the L1 and L2 within two days of incubation (Fig. 2a). In contrast, differences in σ_{PSII} between treatments were not statistically significant (Table S6).

3.2.2. Indicators of growth

The growth rates derived from changes in chl-a were mostly similar to those derived from POC (Figs. 3a, 5a) and the changes in POC and chl-a concentrations were linearly correlated (Figure S3, $p < 0.01$). Chl-a derived growth is therefore considered to be a robust representation of the changes in phytoplankton growth. The chl-a concentration in the PFZ (0.12 μg L^{-1} under initial conditions) did not change significantly after incubation under the low light treatments with or without iron enrichment (Fig. 4a). Under high light, the chl-a concentration doubled to 0.25 μg L^{-1} and 0.28 μg L^{-1}, respectively, in the treatments with or without added iron (Fig. 4a) and the Chl a: POC ratio nearly doubled (from 0.007 to 0.013 μg μg; Table S4) with the addition of iron. The changes in the dissolved macronutrient concentrations in the medium generally corresponded to the changes in chl-a and POC, with stronger nutrient depletion observed where chl-a and POC increased (Table S5).

Phaeopigments (i.e. the sum of phaeophytin-a and phaeophorbide-a) are used in this study to estimate the extent of cell degradation over the course of the incubations. At 46 °S, the initial phaeopigment concentrations were below detection limit and remained below detection in the low light treatment with iron. Phaeopigment:chl-a ratios reached 0.007 μg:μg in the low light treatment without iron, together indicating that degradation was not a major process at low light (Table 2). In

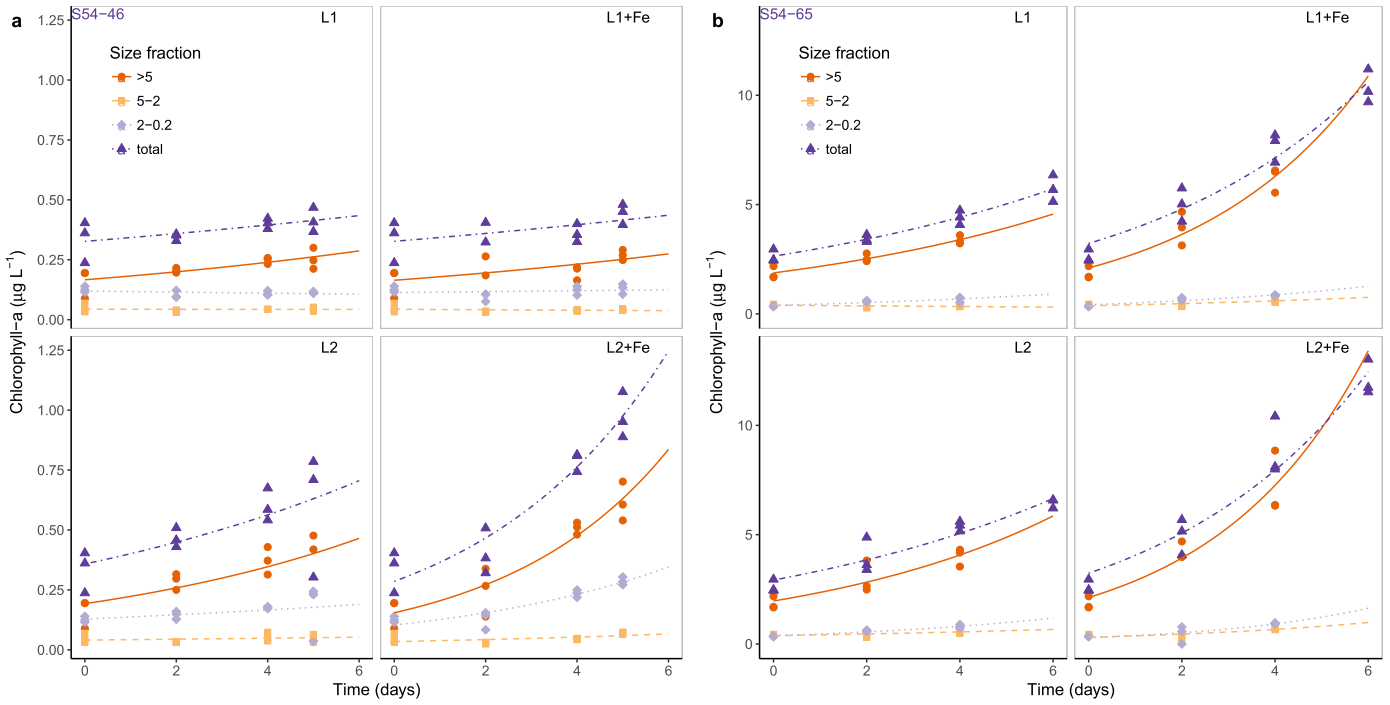

Fig. 3. Changes in size-fractionated chl-a concentrations for incubation experiment S54-46 in the PFZ (a) and incubation experiment S54–65 in the AAZ (b). Size fractionated chl-a concentrations were measured by filtering the samples sequentially through polycarbonate filters with 5, 2 and 0.2 µm pore sizes. The symbols represent individual measurements at each time point (termination). The dotted lines are exponential fits through these individual measurement points.

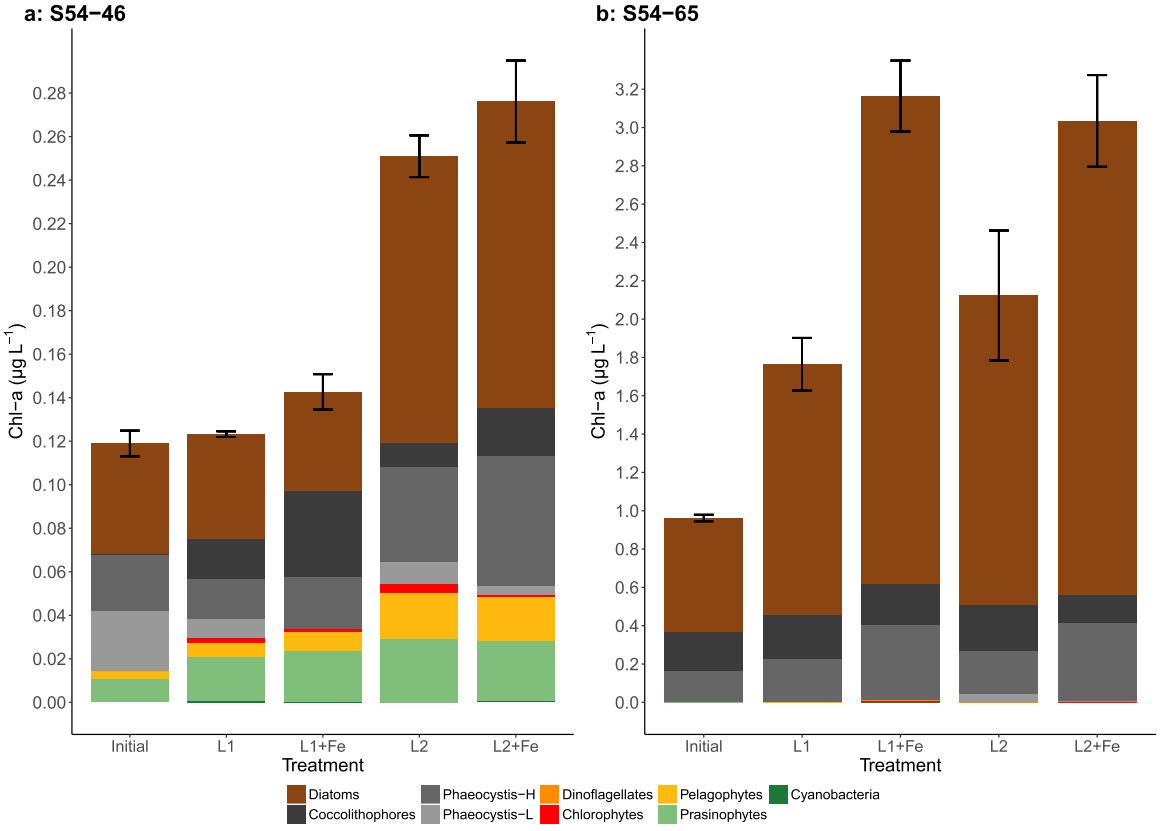

Fig. 4. Phytoplankton composition at the end of each treatment for (a) incubation experiment S54-46 in the PFZ and (b) incubation experiment S54–65 in the AAZ. Initial = Initial community with no treatment; L1 = low light; L2 = high light; +Fe = iron enrichment. Graphs were plotted using the CHEMTAX output results shown in Table S3. Note that due to pigment changes during the incubation, contribution of coccolithophores (pigment category haptophytes Type 6, Zapata et al., 2004) may be overestimated due to contribution of other haptophytes, e.g. Phaeocystis (pigment category haptophytes Type 8, Zapata et al., 2004). A 100% stacked bar chart is shown in Fig. S4, Supplemental information. Error bars represent standard deviations.

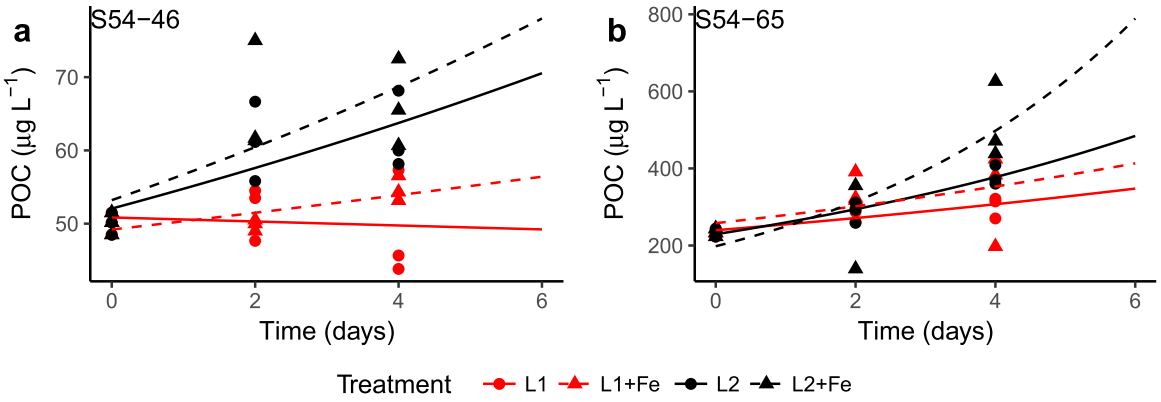

Fig. 5. Changes in particulate organic carbon (POC) concentrations over the course of the two summer 2015 bioassays: S54-46 in the PFZ (a), and S54–65 in the AAZ (b). The red lines indicate the low light treatments (L1; Table 1) and the black lines the higher light treatments (L2; Table 1). Dashed lines and triangles are for iron enriched treatments (+Fe) while solid lines and circles indicate control conditions without iron enrichment. The symbols represent individual measurements at each time point (termination). The lines are exponential fits through these individual measurement points. The y-axes for POC (a,b) are shown on different scales due to the large differences between the two experiments.

Table 2
Ratios of photoprotective versus chl-a and accessory light harvesting pigments in both incubation experiments in response to iron and/or light addition. Phaeo = Phaeopigments, DDT = diadinoxanthin + diatoxanthin (photoprotective), FH = Fuco + Hex (light-harvesting). Detailed data sets (e.g. individual pigment concentrations) can be found in Supplemental Table S9.

	46°S (PFZ)			65°S (AAZ)		
	Phaeo:Chla	DDT:Chla	DDT:FH	Phaeo:Chla	DDT:Chla	DDT:FH
Initial	0.0000	0.069	0.075	0.101	0.051	0.050
L1	0.007	0.066	0.087	0.096	0.054	0.056
L1 + Fe	0.000	0.063	0.092	0.122	0.040	0.046
L2	0.022	0.083	0.122	0.163	0.055	0.065
L2 + Fe	0.022	0.087	0.120	0.286	0.021	0.028

contrast, phaeopigment:chl-a ratios increased up to 0.022 µg:µg under high light, where only phaeophytin-a was detected; phaeophorbide-a was below detection (Table S9). While we cannot exclude the possibility of grazing, especially by microheterotrophs, these low and treatment-specific phaeopigment:chl-a ratios at least point to minor crustacean grazing impacts in our incubations.

3.2.3. Shifts in the community composition

The largest cell fraction (> 5 µm) showed strongest growth in all treatments from 48% to around 61–63% of total chl-a at the end of the incubations (Fig. 3a). In contrast, the contribution of the 0–2 µm fraction decreased to 28–30% and that of the 2–5 µm fraction decreased to 7–11% (Fig. 3a). These shifts in the community at 46 °S were, however, almost the same across all treatments, independent of the light and iron availability implying that neither iron nor light induced particular shifts in the size fractions of the community (Fig. 3a).

The initial composition in the PFZ incubation was dominated by contribution of diatoms along with Phaeocystis. Coccolithophore contribution to chl-a was rather insignificant (Fig. 4a). Under low light conditions, especially after iron enrichment (L1 + Fe), an increase in the contribution of coccolithophores and a decrease in contribution of Phaeocystis and diatoms was observed (Fig. 4a). The relative contribution of coccolithophores may have been overestimated in the low light incubations, as pigment ratios may have changed over the time of incubation leading CHEMTAX to reassign some contribution of other haptophytes to coccolithophores. Both high light treatments (L2 and L2 + Fe) showed an increase in contributions of diatoms to more than 50%, and a decrease in the contribution of Phaeocystis (Fig. 4a). This corresponds to our observation that the largest size group (> 5 µm) showed the strongest increase in chl-a over the course of the high light incubations (Fig. 3).

The contribution of Phaeocystis to chl-a, in general, decreased under low light conditions compared to the initial conditions. However, the response of Phaeocystis acclimated to high iron availability and those acclimated to low iron availability (see 2.4 CHEMTAX set-up) was different. After iron enrichment, contributions (to the total chl-a) of Phaeocystis with a pigment composition indicating low iron availability ("Phaeocystis-L" in Fig. 4) dropped drastically from 23% to non-detectable amounts. Contributions (to the total chl-a) of Phaeocystis with a pigment composition indicating high iron availability ("Phaeocystis-H" in Fig. 4) only decreased from 22% to 17% after iron enrichment.

3.2.4. Photoacclimation

Xanthophyll cycle pigments diadinoxanthin and diatoxanthin (DDT) are further used to assess stress and photo-acclimation strategies in this study. These are found in all of the taxa considered in this paper except chlorophytes, prasinophytes and cyanobacteria (Brunet et al., 2011; Olaizola et al., 1994), and are synthesized to protect the cell against excess light. In the PFZ, the DDT concentration as well as the ratio of DDT (photoprotective pigments) to chl-a and to light harvesting pigments fucoxanthin and 19'-hexanoyloxyfucoxanthin (Fuco + Hex; Fig. S5a), increased in both high light treatments irrespective of iron enrichment (Table 2). This increase in photoprotective pigments was accompanied by an increase in the photosynthetic efficiency (Fv/Fm) especially under conditions of high light with iron enrichment (Fig. S6).

3.3. Responses to increasing iron and light in the AAZ (65 °S)

3.3.1. Indicators of stress relief

All treatments in the AAZ showed an initial increase in Fv/Fm over the course of the incubation (Fig. 2c), matching the changes observed in chl-a and POC-derived growth (Figs. 3 and 5). It is possible that there was a small amount of iron introduced from large cells, including protozoa, disrupted by the 200 µm net filtration, sufficient to temporarily relieve iron limitation even in the control treatments, but which was quickly used by Day 4. Experimental (1 nM) iron addition resulted in strong chl-a and POC increase and similarly, experimental iron addition led to stronger initial increases in Fv/Fm compared to the non-amended treatments (Fig. 2c). After two days the increase in Fv/Fm reached a plateau and then began to decrease. The largest decreases occurred in the non-amended control treatments without iron addition (Fig. 2c). The σ_{PSII} decreased for all treatments during the initial 2–3 days with the greatest decreases occurring in the iron enriched treatments (Fig. 2d).

3.3.2. Indicators of growth

In contrast to the incubations in the PFZ at 46 °S, the experiment at 65 °S in the AAZ showed a major increase in chl-a upon iron enrichment even at the lower light intensity (Fig. 4b). The daily change in chl-a concentration under L2 + Fe conditions at 65 °S was more than three times greater than under L1 conditions (Table S5) resulting in statistically significant differences in chl-a concentrations at the end of the incubations between L1 and L2 + Fe (Table S7, S8). The POC content remained unchanged under low light even after iron enrichment, and consequently, the chl-a:POC ratios more than doubled upon iron enrichment under low light conditions (Table S4). In contrast, POC content increased under high light (Fig. 5), even without iron addition resulting in lower chl-a: POC ratios. Increased nutrient uptake rates were also observed at 65 °S upon iron enrichment under low and high light (Table S5). The strongest silicic acid uptake increase was observed under high light, high iron conditions and the weakest under high light without iron enrichment (L2; Table S4). A noticeable increase in the phaeopigment:chl-a ratios was also observed, especially at L2 + Fe (0.29 μg:μg; Table 2), with generally higher phaeophorbide-a than phaeophytin-a concentrations (Table S9).

3.3.3. Shifts in the community composition

The chl-a derived growth rate was higher in the iron enriched incubations both under low and high light conditions (Fig. 3b). This strong response to iron enrichment can mostly be attributed to the large cells' response (Fig. 3b). Iron enrichment thus seemed to affect both total chl-a concentration as well as community structure in the AAZ independent of the light level. Under all treatments, the increase in total chl-a was mostly due to growth of diatoms (Fig. 4b). Between the treatments, diatom growth was strongest upon iron enrichment: The contribution of diatoms to total chl-a increased to more than 80% with iron enrichment under low and high light (Fig. 4b). Phaeocystis (predominantly the high iron acclimated form) chl-a also increased upon iron enrichment compared to the non-amended treatments (up to 0.4 μg L^{-1}; Fig. 4b), which, however resulted in only minor changes in Phaeocystis contribution to total chl-a (ca. 12% in all treatments; Fig. S4). Coccolithophores responded differently. Lower coccolithophore chl-a concentrations were observed under low light iron enriched treatments compared to the un-amended treatments, decreasing coccolithophores' contribution to total chl-a to ca. 7% upon iron addition (Fig. 4b). The contribution of all other smaller phytoplankton groups was minimal for all treatments in the AAZ. This is in agreement with the chl-a size fractionated measurements, which showed iron enrichment induced major changes in the large size fraction of the community in the AAZ incubations.

3.3.4. Photoacclimation

The DDT (diadinoxanthin + diatoxanthin) photoprotective pigment ratios to chl-a were relatively low in our AAZ incubations (Table 2), with lowest DDT:chl-a ratios observed under the high light treatment with iron (0.021 μg:μg; L2 + Fe). This corresponds to a low DDT:(Fuco + Hex) ratio of 0.028 μg:μg (Table 2), indicating that the community favoured photosynthesis over photoprotection after iron addition at high light.

4. Discussion

The Southern Ocean is not uniform and the response of phytoplankton to the environment in which they live varies between regions (Boyd et al., 2010; Thomalla et al., 2011). This highlights the importance of understanding the factors that drive phytoplankton growth in different regions. Here we focus on the community response to iron and light variability in the Atlantic Sector of the Southern Ocean. The in-situ conditions varied largely between the stations at 46 °S and 65 °S. Hence, pre-adaptation and pre-acclimation (Flynn et al., 2015) of the phytoplankton communities incubated in our experiments were expected to differ.

4.1. Initial differences in environmental conditions, community distribution and acclimation

4.1.1. Environmental conditions

At 65 °S (AAZ), the phytoplankton were exposed to in-situ temperatures close to freezing point, long day-lengths and high nitrate and silicic acid concentrations (Table 1). At 46 °S (PFZ) phytoplankton were exposed to higher in-situ temperatures, shorter day-lengths, and lower silicic acid concentrations than in the AAZ. The mixed layer depth was deep (89 m) at 46 °S, but relatively shallow (31 m) at 65 °S. The station at 65 °S was located within the seasonal ice zone of the AAZ. Based on satellite imagery (Cavalieri et al., 1996, updated yearly), the ice melted relatively late during the summer of 2015 at this location (Fig. S7). This late ice melt might have caused the observed particularly shallow mixing regime and possible micronutrient release.

While surface waters of the summertime Southern Ocean in general are typically iron limited (Moore et al., 2013), Klunder et al. (2011) observed dFe concentrations that decreased southwards along the Good Hope Line in February-March 2008. Our measured dFe concentrations in January 2015 of 0.31 nM at 46 °S and 0.19 nM at 65 °S were in agreement with the range reported by Klunder et al. (2011) for surface waters. Iron limitation is also indicated for both stations by the dFe:NO_3 ratio of 0.016 (nmol:μmol) at 46 °S and 0.0075 (nmol:μmol) at 65 °S, much lower than the ratio of 0.5 (nmol:μmol) based on the global extended Redfield ratio of $(C_{106}N_{16}P_1)_{x1000}Fe_8$ (Morel et al., 2003), and on iron requirements that is about 10-fold lower for Antarctic diatoms compared to temperate species (Strzepek et al., 2012). It is possible that the temperature minimum at approximately 50 m at 65 °S reflects remnant winter water left over from deep water entrainment. The dFe concentration at 50 m was 0.23 nM, slightly higher than the surface concentration of 0.19 nM. Therefore it is possible that the phytoplankton community relies on the upward diffusion of trace metals from this winter layer. Several factors indicate, however, that the iron depletion at 65 °S was likely a recent occurrence following the utilisation of micronutrients released from the melting sea ice that prevailed at at 65 °S until a week before sampling (Fig. S7). For instance, Fv/Fm values were low and indicated iron stress. However, only high-iron acclimated Phaeocystis forms and a relatively high chla:POC ratio were observed at 65 °S, which is rather indicative of iron replete conditions. The pigment acclimation reportedly requires time lags of two or more days between iron addition and biological response (Coale et al., 2003; Sedwick et al., 2007, 2000). Altogether, this would indicate that the initial community at 65 °S was sampled towards the end of a recent bloom caused by ice melt. This recent bloom arguably removed most of the released available dFe and started inducing iron limitation.

4.1.2. Community structure

Varying environmental conditions in the two investigated Southern Ocean water masses not only drive variability in biomass and primary productivity but also in community composition. Shifts in the community composition are important as they change the composition of exported organic matter and the trajectory of primary production through the food web (Boyd and Trull, 2007; Finkel et al., 2010). In our study, picophytoplankton (0–2 μm) played a major role (38% of total chl-a) in the PFZ, while diatoms and non-calcified haptophytes (Phaeocystis) both contributed less than 45% each to the total chl-a, corresponding to previous findings in the Polar Frontal and Subantarctic waters (e.g., Gervais et al., 2002; Ishikawa et al., 2002). This indicates that the PFZ community was more diverse, possibly due the deep mixed layer which in turn also caused the community to be more light than iron limited, as discussed further below. In the AAZ, in contrast, the phytoplankton community was dominated by large

(> 5 μm) cells. The CHEMTAX analyses revealed that diatoms largely dominated (ca. 60% w.r.t. chl-a) this phytoplankton community despite the observed low dFe concentration and very low dFe:NO_3 ratios. Either the diatom growth had only recently induced the iron depletion, and/or secondary factors such as depth of vertical mixing might have played a key role here, favouring large cells in the shallow mixed layer of the Antarctic waters (Swan et al., 2015; Wright et al., 2010). Some nanoplanktonic sea-ice diatom species such as *Fragilariopsis cylindrus* can also grow with minimal iron availability by replacing ferridoxin with flavodoxin (Pankowski and Mcminn, 2009). Higher silicic acid availability in the AAZ, necessary for diatom growth, is also likely to have affected the in-situ community composition. Strong grazing pressure is unlikely given the low phaeopigment:chl-a ratios.

4.1.3. Photophysiology and acclimation

We observed low initial photosynthetic efficiencies (Fv/Fm) at 46 °S and at 65 °S, which could indicate iron limitation in both water masses. Additionally, it could be due to region-specific causes: 1) light inhibition during daytime (due to the shallow mixed layer) in the AAZ, and 2) larger contribution of smaller phytoplankton in the PFZ. Our data set does not allow for disentangling these interacting driving forces. Light inhibition in the AAZ might have resulted from the observed lower photoprotective versus assimilatory pigments ratio. The initial average σ_{PSII} ($7.9\,nm^{-2}$ quanta^{-1}) at 65 °S was only slightly lower than the range observed in laboratory Southern Ocean diatom cultures, but higher than published values for coastal diatoms isolates (Strzepek et al., 2012) and much higher than at 46 °S ($2.8\,nm^{-2}$ quanta^{-1}). As photoinhibition was unlikely at the depth of sampling in the AAZ, this relatively high σ_{PSII} may be a result of the pre-acclimation to very low iron availability. Shifts in the phytoplankton community may also influence the σ_{PSII} (Suggett et al., 2004). However, as mentioned above, the PFZ contained a more diverse functional community, including prasinophytes and pelagophytes, for example. Prasinophytes and pelagophytes have much larger absorption cross sections compared to diatoms (Suggett et al., 2004), which means that we should expect larger σ_{PSII} in the PFZ if the σ_{PSII} was mainly driven by the community composition. Since this is not the case, photoacclimation appears to better explain the larger σ_{PSII} observed in our study in the AAZ compared to the PFZ.

4.2. Growth and community structure response to enrichment in iron and light

The differences in environmental conditions, community composition and acclimation, resulted in different responses to relief of iron and light limitation. The community at 46 °S was slightly enhanced by iron enrichment in low light conditions, but much stronger if the light environment was suitable. This would indicate a dependent co-limitation (Saito et al., 2008), where light is the primary limiting factor. In the ocean, such conditions would, for example, arise after a resupply of iron through deep mixing followed by a shoaling of the mixed layer. Inability of Southern Ocean phytoplankton to use the external supply of iron under unfavourable light conditions has been observed previously in areas with deep mixed layers (Cassar et al., 2011; de Baar et al., 2005). For temperate phytoplankton, Sunda and Huntsman (1997) suggested that iron enrichment might relieve light limitation as the greater requirement for photosynthetic iron-based redox proteins in low-light acclimatized algae can be met. In contrast, our findings at 46 °S, a mixed community, support Strzepek et al.'s (2012) observations that iron enrichment does not always provide relief of light limitation and that the response to iron and light availability in Southern Ocean Subantarctic communities may differ from temperate phytoplankton.

However, at 65 °S, a diatom dominated community, iron enrichment indeed led to increased growth even at low light. The greater macronutrient depletion observed in our AAZ incubation media upon iron enrichment supports the assumption that the AAZ community insufficiently consumes macronutrients under iron limiting conditions explaining the prevailing excess macronutrient availability in Antarctic waters, and that only iron enrichment enables an increased utilisation of macronutrients. Additional light, without iron enrichment resulted in low chl-a increase. This points towards a dependent co-limitation where iron is the predominant factor. The phytoplankton in the AAZ might only be light limited if iron limits the restructuring of the photosynthetic apparatus. The contrasting response of the phytoplankton community at 46 °S and 65 °S indicates that the potential to use iron enrichment under low light conditions mainly depends on the resident phytoplankton assemblage and pre-acclimation.

The changes observed in the community composition over the course of the incubations, provide further insight into which functional groups benefited most. At 65 °S, diatoms' contribution to total chl-a increased in all treatments, most so (up to 80%) upon iron enrichment independent of the light regime in agreement with previous studies, which showed that large diatoms benefited the most from sudden iron enrichment (Hoffmann et al., 2006 and references therein). Our observations in the PFZ were different though. The size-fractionated composition in the PFZ barely changed over the course of the six day long incubation, independent of the treatment. At this site, diatoms only increased their contribution to total chl-a under high light conditions (from 43% up to 52%). Under low light conditions, the contribution of coccolithophores to total chl-a increased (from 0.3% to 28%) whereas the contribution of diatoms and Phaeocystis decreased. Nonetheless, the observed shift in the pigment composition from Phaeocystis acclimated to high iron availability to Phaeocystis acclimated to low iron availability in the PFZ supports the Deppeler and Davidson (2017) assumption of the great potential of *P. antarctica* to thrive in the future oceans.

4.3. Photophysiological changes in response to changes in iron and light

Changes in the cellular chl-a content are usually part of the acclimation strategies to changes in light and nutrient regimes (Behrenfeld et al., 2005). Under light limitation, one widespread acclimation strategy in phytoplankton is to increase the cellular chl-a content so that additional photosynthetic units (PSU) can be synthesized and maximum light can be captured. However, the synthesis of these units requires iron and hence the iron demand is increased under light limiting conditions. Under iron limitation on the other hand, phytoplankton are unable to produce enough PSU to capture sufficient light for photosynthesis and growth (Sunda and Huntsman, 1997). Therefore, generally, iron-replete phytoplankton are known to have higher chl-a:POC ratios than iron depleted cells (Moore et al., 2007), while increased light availability generally results in a decrease in chl-a:POC ratios. In line with this, the chl-a:POC ratio increased in the AAZ upon iron enrichment, especially under low light conditions, but in the PFZ the ratio only increased upon iron enrichment and high light conditions (Table S4). Hence, similar to observations for growth, the change in the photosynthetic apparatus, specifically in cellular chl-a, appears to occur upon relief of iron limitation alone in the AAZ, while such changes require relief of both iron and light limitation in the PFZ.

Diatoms and haptophytes (Phaeocystis and coccolithophores) present an additional acclimation strategy to varying light intensities whereby they use pigments of the xanthophyll cycle, such as diadinoxanthin and diatoxanthin, for photoprotection (Brunet et al., 2011). Our PFZ experiment showed, as in Moore et al. (2007), that increases in light caused increases in the concentration of photoprotective pigments. However, this did not occur in the AAZ, despite the dominance of xanthophyll producing phytoplankton groups, diatoms and haptophytes. They were either not able to produce sufficient amounts of photoprotective pigments or used other protective strategies. The increase in chl-a degradation products (phaeopigments, especially phaeophorbide-a) under high light conditions suggests that the AAZ community might have been limited in their capacity to prevent photo-

inhibition and resulting cell damage and chl-a degradation.

Typically, in the world's oceans, phytoplankton iron requirements are lower under higher irradiance than under lower irradiances. Strzepek et al. (2012), however, suggested that Southern Ocean phytoplankton – in contrast to temperate communities - respond to low light by increasing the size of PSU rather than the number of PSU. As a result, their demand for iron is not increased to the same extent under low light as they do not require extra iron to build new PSU. Hence, they might not be iron deficient when they are acclimated to low light. Strzepek et al. (2012) furthermore suggested that the increased size of PSU is reflected in high σ_{PSII} values. However, contrary to Strzepek et al. (2012) findings, the σ_{PSII} did not change noticeably over the course of our PFZ incubations (Fig. 2b). This might be due to a lack of short-term response in the size of PSU in our six days long incubations, or to the observed shifts in the community. At 65 ˚S, in the AAZ, however, iron enrichment did lead to strong growth and an increase in Fv/Fm values under low light intensities compared to the non-amended treatment. The σ_{PSII} decreased in all treatments over the course of the incubation, but most dramatically so in the iron enriched incubations. Fv/Fm showed an inverse response, with most drastic increase in the iron enriched incubations. The decrease in Fv/Fm at a later stage during the incubations, especially in the non-iron amended treatments may indicate photoinhibition, potentially a result of the above mentioned low photoprotective versus assimilatory pigment ratios in the AAZ.

5. Conclusion

In this study, two incubation experiments were conducted showing responses of Southern Ocean phytoplankton to iron enrichment and higher irradiances. As had been suggested previously, a dependent co-limitation of iron and light in both water masses was confirmed. However, the importance of one or the other limiting factor was shown to differ regionally. The community in the PFZ showed a stronger response to light than to iron, while in the AAZ, iron was the dominant limiting factor. The latter was attributed to differences in the resident community as well as to pre-acclimation to post-bloom and a shallower surface mixed layer. At both sites, however, addition of both iron and light led to the strongest responses in chl-a, POC and photochemical efficiency, indicating that iron and light in both water masses to some extent in both locations co-limited phytoplankton photosynthesis and growth. Iron and light addition not only induced changes in growth and photochemical efficiency, but also resulted in important shifts in community structure. For example, at 46 ˚S, where the functional diversity was higher than at 65 ˚S, coccolithophore and prasinophytes contributions were higher under low light than under high light, independent of the iron addition, whereas the diatom contribution was lower under low light and higher under high light. At 65 ˚S in contrast, diatom contribution increased more upon iron enrichment than under high light alone. Such changes in the phytoplankton community will have major consequences on the macronutrient and carbon cycles at the ocean surface, as well as on the sinking and settling of calcium carbonate and silicate. The knowledge of region-specific responses in growth, photochemical efficiency and community composition is therefore key to improve biogeochemical models and the understanding of our future oceans.

Acknowledgements

The work leading to these results received funding from the National Research Foundation, South Africa (NRF), under the SA/Norway Collaboration Programme and the South African National Antarctic Programme, Grant nos. 91313 and 110731 awarded to S.F. R.P. acknowledges support from NRF-South Africa through a SANCOR-NRF fellowship under Grant no. 94915. J.V. acknowledges funding from NRF-South Africa through a Masters Innovation Scholarship. The XBT data used in this manuscript are made freely available on the Atlantic Oceanographic and Meteorological Laboratory and are funded by the NOAA Office of Climate Observations, USA. The authors thank NASA Goddard Space Flight Center, Ocean Ecology Laboratory, Ocean Biology Processing Group, for seasonal composite chl-a concentrations. The authors furthermore thank Smit Amandla crew of the R/V SA Agulhas II, Department of Environmental Affairs (DEA), and all the scientific cruise participants of SANAE 54. The authors greatly acknowledge the valuable contributions of three anonymous reviewers.

Appendix A. Supplementary material

Supplementary data associated with this article can be found in the online version at doi:10.1016/j.dsr.2018.09.006.

References

Alderkamp, A.C., Mills, M.M., van Dijken, G.L., Laan, P., Thuróczy, C.E., Gerringa, L.J.A., de Baar, H.J.W., Payne, C.D., Visser, R.J.W., Buma, A.G.J., Arrigo, K.R., 2012. Iron from melting glaciers fuels phytoplankton blooms in the Amundsen Sea (Southern Ocean): phytoplankton characteristics and productivity. Deep Sea Res. II 71–76, 32–48. https://doi.org/10.1016/j.dsr2.2012.03.005.

Behrenfeld, M.J., Boss, E., Siegel, D.A., Shea, D.M., 2005. Carbon-based ocean productivity and phytoplankton physiology from space. Glob. Biogeochem. Cycles 19, 1–14. https://doi.org/10.1029/2004GB002299.

Behrenfeld, M.J., Milligan, A.J., 2013. Photophysiological expressions of iron stress in phytoplankton. Ann. Rev. Mar. Sci. 5, 217–246. https://doi.org/10.1146/annurev-marine-121211-172356.

Billany, W., Swart, S., Hermes, J., Reason, C.J.C., 2010. Variability of the Southern Ocean fronts at the Greenwich Meridian. J. Mar. Syst. 82, 304–310. https://doi.org/10.1016/j.jmarsys.2010.06.005.

Boyd, P.W., Abraham, E.R., 2001. Iron-mediated changes in phytoplankton photosynthetic competence during SOIREE. Deep Sea Res. II 48, 2529–2550. https://doi.org/10.1016/S0967-0645(01)00007-8.

Boyd, P.W., Ellwood, M.J., 2010. The biogeochemical cycle of iron in the ocean. Nat. Geosci. 3, 675–682. https://doi.org/10.1038/ngeo964.

Boyd, P.W., Strzepek, R., Fu, F., Hutchins, D.A., 2010. Environmental control of open-ocean phytoplankton groups: now and in the future. Limnol. Oceanogr. 55, 1353–1376. https://doi.org/10.4319/lo.2010.55.3.1353.

Boyd, P.W., Trull, T.W., 2007. Understanding the export of biogenic particles in oceanic waters: is there consensus? Prog. Oceanogr. 72, 276–312. https://doi.org/10.1016/j.pocean.2006.10.007.

Boyd, P.W., Watson, A.J., Law, C.S., Abraham, E.R., Trull, T., Murdoch, R., Bakker, D.C.E., Bowie, A.R., Buesseler, K.O., Chang, H., Charette, M., Croot, P., Downing, K., Frew, R., Gall, M., Hadfield, M., Hall, J., Harvey, M., Jameson, G., LaRoche, J., Liddicoat, M., Ling, R., Maldonado, M.T., McKay, R.M., Nodder, S., Pickmere, S., Pridmore, R., Rintoul, S., Safi, K., Sutton, P., Strzepek, R., Tanneberger, K., Turner, S., Waite, A., Zeldis, J., 2000. A mesoscale phytoplankton bloom in the polar Southern Ocean stimulated by iron fertilization. Nature 407, 695–702. https://doi.org/10.1038/35037500.

Boyer, T.P., Antonov, J.I., Baranova, O.K., Coleman, C., Garcia, H.E., Grodsky, A., Johnson, D.R., Locarnini, R.A., Mishonov, A.V., O'Brien, T.D., Paver, C.R., Reagan, J. R., Seidov, D., Smolyar, I.V., Zweng, M.M., 2013. World Ocean Database 2013. NOAA Atlas NESDIS 72, Silver Spring, MD.

Brunet, C., Johnsen, G., Lavaud, J., Roy, S., 2011. Pigments and photoacclimation processes. In: Roy, S., Llewellyn, C., Egeland, E.S., Johnsen, G. (Eds.), Phytoplankton Pigments: Characterization, Chemotaxonomy and Applications in Oceanography. Cambridge University Press, New York, pp. 445–471. https://doi.org/10.1017/CBO9780511732263.017.

Carter, L., McCave, I.N., Williams, M.J.M., 2008. Chapter 4 circulation and water masses of the Southern Ocean: a review. Dev. Earth Environ. Sci. 8, 85–114. https://doi.org/10.1016/S1571-9197(08)00004-9.

Cassar, N., DiFiore, P.J., Barnett, B.A., Bender, M.L., Bowie, A.R., Tilbrook, B., Petrou, K., Westwood, K.J., Wright, S.W., Lefevre, D., 2011. The influence of iron and light on net community production in the Subantarctic and Polar Frontal Zones. Biogeosciences 8, 227–237. https://doi.org/10.5194/bg-8-227-2011.

Cavalieri, D.J., Parkinson, C.L., Gloersen, P., Zwally, H.J., 1996. Sea ice concentrations from Nimbus-7 SMMR and DMSP SSM/I-SSMIS Passive Microwave Data, Version 1. (December 2013 to January 2015 daily data). ⟨https://doi.org/10.5067/8GQ8LZQVL0VL⟩.

Cheah, W., McMinn, A., Griffiths, F.B., Westwood, K.J., Wright, S.W., Clementson, L.A., 2013. Response of phytoplankton photophysiology to varying environmental conditions in the Sub-Antarctic and Polar Frontal Zone. PLoS One 8, e72165. https://doi.org/10.1371/journal.pone.0072165.

Cloete, R., Loock, J.C., Mtshali, T.N., Fietz, S., Roychoudhury, A.N., 2018. Winter and summer distributions of Copper, Zinc and Nickel along the International GEOTRACES section GIPY05: Insights into deep winter mixing. Chem. Geol (revisions submitted) (manuscript nr. CHEMGE-S-18-00174).

Coale, K.H., Johnson, K.S., Chavez, F.P., Buesseler, K.O., Barber, R.T., Brzezinski, M.A., Cochlan, W.P., Millero, F.J., Falkowski, P.G., Bauer, J.E., Wanninkhof, R.H., Kudela, R.M., Altabet, M.A., Hales, B.E., Takahashi, T., Landry, M.R., Bidigare, R.R., Wang, X., Chase, Z., Strutton, P.G., Friederich, G.E., Gorbunov, M.Y., Lance, V.P., Hilting,

A.K., Hiscock, M.R., Demarest, M., Hiscock, W.T., Sullivan, K.F., Tanner, S.J., Gordon, R.M., Hunter, C.N., Elrod, V.A., Fitzwater, S.E., Jones, J.L., Tozzi, S., Koblizek, M., Roberts, A.E., Herndon, J., Brewster, J., Ladizinsky, N., Smith, G., Cooper, D., Timothy, D., Brown, S.L., Selph, K.E., Sheridan, C.C., Twining, B.S., Johnson, Z.I., 2004. Southern ocean iron enrichment experiment: carbon cycling in high- and low-Si waters. Science 304, 408–414. https://doi.org/10.1126/science.1089778.

Coale, K.H., Wang, X., Tanner, S.J., Johnson, K.S., 2003. Phytoplankton growth and biological response to iron and zinc addition in the Ross Sea and Antarctic Circumpolar Current along 170°W. Deep Sea Res. II 50, 635–653. https://doi.org/10.1016/S0967-0645(02)00588-X.

Cutter, G., Codispoti, L., Croot, P., Francois, R., Lohan, M., Rutgers Van Der Loeff, M., 2014. Sampling and Sample-handling Protocols for GEOTRACES Cruises. URL ⟨http://www.geotraces.org/images/stories/documents/intercalibration/Cookbook_v2.pdf⟩ (Accessed 16 January 2018).

Cutter, G.A., Bruland, K.W., 2012. Rapid and noncontaminating sampling system for trace elements in global ocean surveys. Limnol. Oceanogr. Methods 10, 425–436. https://doi.org/10.4319/lom.2012.10.425.

de Baar, H.J.W., Boyd, P.W., Coale, K.H., Landry, M.R., Tsuda, A., Assmy, P., Bakker, D.C.E., Bozec, Y., Barber, R.T., Brzezinski, M.A., Buesseler, K.O., Boyé, M., Croot, P.L., Gervais, F., Gorbunov, M.Y., Harrison, P.J., Hiscock, W.T., Laan, P., Lancelot, C., Law, C.S., Levasseur, M., Marchetti, A., Millero, F.J., Nishioka, J., Nojiri, Y., van Oijen, T., Riebesell, U., Rijkenberg, M.J.A., Saito, H., Takeda, S., Timmermans, K.R., Veldhuis, M.J.W., Waite, A.M., Wong, C., 2005. Synthesis of iron fertilization experiments: from the iron age in the age of enlightenment. J. Geophys. Res. 110, C09S16. https://doi.org/10.1029/2004JC002601.

de Baar, H.J.W., Buma, A.G.J., Nolting, R.F., Cadee, G.C., Jacques, G., Treguer, P.J., 1990. On iron limitation of the Southern Ocean: experimental observations in the Weddell and Scotia Seas. Mar. Ecol. Prog. Ser. 65, 105–122. https://doi.org/10.3354/meps065105.

de Boyer Montégut, C., Madec, G., Fischer, A.S., Lazar, A., Iudicone, D., 2004. Mixed layer depth over the global ocean: an examination of profile data and a profile-based climatology. J. Geophys. Res. C Ocean 109, 1–20. https://doi.org/10.1029/2004JC002378.

Deppeler, S.L., Davidson, A.T., 2017. Southern Ocean Phytoplankton in a changing climate. Front. Mar. Sci. 4, 40. https://doi.org/10.3389/fmars.2017.00040.

DiTullio, G.R., Garcia, N., Riseman, S.F., Sedwick, P.N., 2007. Effects of iron concentration on pigment composition in Phaeocystis antarctica grown at low irradiance. Biogeochemistry 83, 71–81. https://doi.org/10.1007/978-1-4020-6214-8_7.

Egan, L., 2008. Determination of Nitrate and/or Nitrite in Brackish or Seawater by Flow Injection Analysis. QuikChem® Method 31-107-04-1-C. Lachat Instruments, USA.

Feng, Y., Hare, C.E., Rose, J.M., Handy, S.M., DiTullio, G.R., Lee, P.A., Smith, W.O., Peloquin, J., Tozzi, S., Sun, J., Zhang, Y., Dunbar, R.B., Long, M.C., Sohst, B., Lohan, M., Hutchins, D.A., 2010. Interactive effects of iron, irradiance and CO_2 on Ross Sea phytoplankton. Deep Sea Res. I 57, 368–383. https://doi.org/10.1016/j.dsr.2009.10.013.

Finkel, Z.V., Beardall, J., Flynn, K.J., Quigg, A., Rees, T.A.V., Raven, J.A., 2010. Phytoplankton in a changing world: cell size and elemental stoichiometry. J. Plankton Res. 32, 119–137. https://doi.org/10.1093/plankt/fbp098.

Flynn, K.J., St John, M., Raven, J.A., Skibinski, D.O.F., Allen, J.I., Mitra, A., Hofmann, E.E., 2015. Acclimation, adaptation, traits and trade-offs in plankton functional type models: reconciling terminology for biology and modelling. J. Plankton Res. 37, 683–691. https://doi.org/10.1093/plankt/fbv036.

Gervais, F., Riebesell, U., Gorbunov, M.Y., 2002. Changes in primary productivity and chlorophyll a in response to iron fertilization in the Southern Polar Frontal Zone. Limnol. Oceanogr. 47, 1324–1335. https://doi.org/10.4319/lo.2002.47.5.1324.

Gibberd, M.J., Kean, E., Barlow, R., Thomalla, S., Lucas, M., 2013. Phytoplankton chemotaxonomy in the Atlantic sector of the Southern Ocean during late summer 2009. Deep Sea Res. I 78, 70–78. https://doi.org/10.1016/j.dsr.2013.04.007.

Grasshoff, K., Ehrhardt, M., Kremling, K., Almgren, T., 1983. Methods of Seawater Analysis. Verlag Chemie, Weinheim, Germany.

Hoffmann, L.J., Peeken, I., Lochte, K., Assmy, P., Veldhuis, M., 2006. Different reactions of Southern Ocean phytoplankton size classes to iron fertilization. Limnol. Oceanogr. 51, 1217–1229. https://doi.org/10.4319/lo.2006.51.3.1217.

Howes, E.L., Joos, F., Eakin, C.M., Gattuso, J.-P., 2015. An updated synthesis of the observed and projected impacts of climate change on the chemical, physical and biological processes in the oceans. Front. Mar. Sci. 2, 36. https://doi.org/10.3389/fmars.2015.00036.

Ishikawa, A., Wright, S.W., Enden, R. Van Den, Davidson, A.T., Marchant, H.J., 2002. Abundance, size structure and community composition of phytoplankton in the Southern Ocean in the austral summer 1999/2000. Polar Biosci. 15, 11–26.

Klunder, M.B., Laan, P., Middag, R., De Baar, H.J.W., van Ooijen, J.C., 2011. Dissolved iron in the Southern Ocean (Atlantic sector). Deep Sea Res. II 58, 2678–2694. https://doi.org/10.1016/j.dsr2.2010.10.042.

Lance, V.P., Hiscock, M.R., Hilting, A.K., Stuebe, D.A., Bidigare, R.R., Smith, W.O., Barber, R.T., 2007. Primary productivity, differential size fraction and pigment composition responses in two Southern Ocean in situ iron enrichments. Deep Sea Res. I 54, 747–773. https://doi.org/10.1016/J.DSR.2007.02.008.

Loock, J., Cloete, R., Mtshali, T., Fietz, S., Roychoudhury, A.N., 2018. The biogeochemistry of Co, Mn and Cd on a seasonal re-occupation of the Southern Ocean. Chem. Geol (manuscript nr. CHEMGE-S-18-00176) (revisions submitted).

Mackey, M.D., Mackey, D.J., Higgins, H.W., Wright, S.W., 1996. CHEMTAX - a program for estimating class abundances from chemical markers: application to HPLC measurements of phytoplankton. Mar. Ecol. Prog. Ser. 144, 265–283. https://doi.org/10.3354/meps144265.

Martin, J.H., Gordon, R.M., Fitzwater, S.E., 1990. Iron in Antarctic waters. Nature 345, 156–158. https://doi.org/10.1038/345156a0.

Mendes, C.R.B., Kerr, R., Tavano, V.M., Cavalheiro, F.A., Garcia, C.A.E., Gauns Dessai, D.R., Anilkumar, N., 2015. Cross-front phytoplankton pigments and chemotaxonomic groups in the Indian sector of the Southern Ocean. Deep Sea Res. II 118, 221–232. https://doi.org/10.1016/j.dsr2.2015.01.003.

Mills, M.M., Alderkamp, A.-C., Thuróczy, C.-E., van Dijken, G.L., Laan, P., de Baar, H.J.W., 2012. Phytoplankton biomass and pigment responses to Fe amendments in the Pine Island and Amundsen polynyas. Deep Sea Res. II 71–76, 61–76. https://doi.org/10.1016/J.DSR2.2012.03.008.

Moore, C.M., Mills, M.M., Arrigo, K.R., Berman-Frank, I., Bopp, L., Boyd, P.W., Galbraith, E.D., Geider, R.J., Guieu, C., Jaccard, S.L., Jickells, T.D., La Roche, J., Lenton, T.M., Mahowald, N.M., Marañón, E., Marinov, I., Moore, J.K., Nakatsuka, T., Oschlies, A., Saito, M.A., Thingstad, T.F., Tsuda, A., Ulloa, O., 2013. Processes and patterns of oceanic nutrient limitation. Nat. Geosci. 6, 701–710. https://doi.org/10.1038/ngeo1765.

Moore, C.M., Seeyave, S., Hickman, A.E., Allen, J.T., Lucas, M.I., Planquette, H., Pollard, R.T., Poulton, A.J., 2007. Iron-light interactions during the CROZet natural iron bloom and export experiment (CROZEX) I: phytoplankton growth and photophysiology. Deep Sea Res. II 54, 2045–2065. https://doi.org/10.1016/j.dsr2.2007.06.011.

Morel, F.M.M., Milligan, A.J., Saito, M.A., 2003. Marine bioinorganic chemistry: the role of trace metals in the oceanic cycles of major nutrients. In: Treatise on Geochemistry. Elsevier, pp. 113–143. ⟨https://doi.org/10.1016/B0-08-043751-6/06108-9⟩.

NASA Ocean Biology Processing Group, 2014. VIIRSN Level-3 Standard Mapped Image. Maint. by NASA Ocean Biol. Distrib. Act. Arch. Cent. (OB.DAAC), Goddard Sp. Flight Center, Greenbelt MD. URL ⟨http://oceancolor.gsfc.nasa.gov/cgi/l3⟩ (Accessed 22 June 2016).

NOAA, 2015. High density XBT transects: AX25. URL ⟨http://www.aoml.noaa.gov/phod/hdenxbt/ax_home.php?Ax=25⟩ (Accessed 22 June 2016).

Olaizola, M., La Roche, J., Kolber, Z., Falkowski, P.G., 1994. Non-photochemical fluorescence quenching and the diadinoxanthin cycle in a marine diatom. Photosynth. Res. 41, 357–370. https://doi.org/10.1007/BF00019413.

Orsi, A.H., Whitworth, T., Nowlin, W.D., 1995. On the meridional extent and fronts of the Antarctic Circumpolar Current. Deep Sea Res. I 42, 641–673. https://doi.org/10.1016/0967-0637(95)00021-W.

Pankowski, A., Mcminn, A., 2009. Iron availability regulates growth, photosynthesis, and production of ferredoxin and flavodoxin in Antarctic sea ice diatoms. Aquat. Biol. 4, 273–288. https://doi.org/10.3354/ab00116.

Peloquin, J., Hall, J., Safi, K., Ellwood, M., Law, C.S., Thompson, K., Kuparinen, J., Harvey, M., Pickmere, S., 2011. Control of the phytoplankton response during the SAGE experiment: a synthesis. Deep Sea Res. II 58, 824–838. https://doi.org/10.1016/J.DSR2.2010.10.019.

Petrou, K., Hassler, C.S., Doblin, M.A., Shelly, K., Schoemann, V., van den Enden, R., Wright, S., Ralph, P.J., 2011. Iron-limitation and high light stress on phytoplankton populations from the Australian sub-Antarctic zone (SAZ). Deep Sea Res. II 58, 2200–2211. https://doi.org/10.1016/J.DSR2.2011.05.020.

Petrou, K., Trimborn, S., Rost, B., Ralph, P.J., Hassler, C.S., 2014. The impact of iron limitation on the physiology of the Antarctic diatom Chaetoceros simplex. Mar. Biol. 161, 925–937. https://doi.org/10.1007/s00227-014-2392-z.

Pollard, R.T., Lucas, M.I., Read, J.F., 2002. Physical controls on biogeochemical zonation in the Southern Ocean. Deep Sea Res. II 49, 3289–3305. https://doi.org/10.1016/S0967-0645(02)00084-X.

R Core Team, 2015. R: A Language and Environment for Statistical Computing.

Ras, J., Claustre, H., Uitz, J., 2008. Spatial variability of phytoplankton pigment distributions in the Subtropical South Pacific Ocean: comparison between in situ and predicted data. Biogeosciences 5, 353–369. https://doi.org/10.5194/bgd-4-3409-2007.

Raven, J.A., 1990. Predictions of Mn and Fe use efficiencies of phototrophic growth as a function of light availability for growth and of C assimilation pathway. New Phytol. 116, 1–18. https://doi.org/10.1111/j.1469-8137.1990.tb00505.x.

Saito, M.A., Goepfert, T.J., Ritt, J.T., 2008. Some thoughts three definitions on the concept of colimitation: and the importance of bioavailability. Limnol. Oceanogr. 53, 276–290. https://doi.org/10.4319/lo.2008.53.1.0276.

Schlitzer, R., 2002. Carbon export fluxes in the Southern Ocean: results from inverse modeling and comparison with satellite-based estimates. Deep Sea Res. II 49, 1623–1644. https://doi.org/10.1016/S0967-0645(02)00004-8.

Schlüter, L., Henriksen, P., Nielsen, T.G., Jakobsen, H.H., 2011. Phytoplankton composition and biomass across the southern Indian Ocean. Deep Sea Res. I 58, 546–556. https://doi.org/10.1016/j.dsr.2011.02.007.

Sedwick, P.N., DiTullio, G.R., Mackey, D.J., 2000. Iron and manganese in the Ross Sea, Antarctica: seasonal iron limitation in Antarctic shelf waters. J. Geophys. Res. Ocean. 105, 11321–11336. https://doi.org/10.1029/2000JC000256.

Sedwick, P.N., Garcia, N.S., Riseman, S.F., Marsay, C.M., DiTullio, G.R., 2007. Evidence for high iron requirements of colonial Phaeocystis antarctica at low irradiance. Biogeochemistry 83, 83–97. https://doi.org/10.1007/s10533-007-9081-7.

Strzepek, R.F., Harrison, P.J., 2004. Photosynthetic architecture differs in coastal and oceanic diatoms. Nature 431, 689–692. https://doi.org/10.1038/nature02954.

Strzepek, R.F., Hunter, K.A., Frew, R.D., Harrison, P.J., Boyd, P.W., 2012. Iron-light interactions differ in Southern Ocean phytoplankton. Limnol. Oceanogr. 57, 1182–1200. https://doi.org/10.4319/lo.2012.57.4.1182.

Suggett, D.J., MacIntyre, H.L., Geider, R.J., 2004. Evaluation of biophysical and optical determinations of light absorption by photosystem II in phytoplankton. Limnol. Oceanogr. Methods 2, 316–332. https://doi.org/10.4319/lom.2004.2.316.

Sunda, W.G., 1997. Control of dissolved iron concentrations in the world ocean, A comment. Mar. Chem. 57, 169–172. https://doi.org/10.1016/S0304-4203(97)00045-5.

Sunda, W.G., Huntsman, S.A., 1997. Interrelated influence of iron, light and cell size on marine phytoplankton growth light and cell size on marine. Nature 2051, 389–392. https://doi.org/10.1038/37093.

Swan, C.M., Vogt, M., Gruber, N., Laufkoetter, C., 2015. A global seasonal surface ocean climatology of phytoplankton types based on CHEMTAX analysis of HPLC pigments. Deep Sea Res. I. https://doi.org/10.1016/j.dsr.2015.12.002.

Thomalla, S.J., Fauchereau, N., Swart, S., Monteiro, P.M.S., 2011. Regional scale characteristics of the seasonal cycle of chlorophyll in the Southern Ocean. Biogeosciences 8, 2849–2866. https://doi.org/10.5194/bg-8-2849-2011.

Timmermans, K.R., Davey, M.S., Van der Wagt, B., Snoek, J., Geider, R.J., Veldhuis, M.J.W., Gerringa, L.J.A., De Baar, H.J.W., 2001. Co-limitation by iron and light of Chaetoceros brevis, C. dichaeta and C. calcitrans (Bacillariophyceae). Mar. Ecol. Prog. Ser. 217, 287–297. https://doi.org/10.3354/meps217287.

Timmermans, K.R., Van Der Wagt, B., Veldhuis, M.J.W., Maatman, A., De Baar, H.J.W., 2005. Physiological responses of three species of marine pico-phytoplankton to ammonium, phosphate, iron and light limitation. J. Sea Res. 53, 109–120. https://doi.org/10.1016/j.seares.2004.05.003.

van Oijen, T., van Leeuwe, M.A., Granum, E., Weissing, F.J., Bellerby, R.G.J., Gieskes, W.W.C., de Baar, H.J.W., 2004. Light rather than iron controls photosynthate production and allocation in Southern Ocean phytoplankton populations during austral autumn. J. Plankton Res. 26, 885–900. https://doi.org/10.1093/plankt/fbh088.

Wickham, H., 2009. Ggplot2: Elegant Graphics for Data Analysis. Springer-Verlag, New York.

Wolters, M., 2002. Determination of Silicate in Brackish or Seawater by Flow Injection Analysis. QuikChem® Method 31-114-27-1-D. Lachat Instruments, USA.

Wright, S.W., van den Enden, R.L., Pearce, I., Davidson, A.T., Scott, F.J., Westwood, K.J., 2010. Phytoplankton community structure and stocks in the Southern Ocean (30-80E) determined by CHEMTAX analysis of HPLC pigment signatures. Deep Sea Res. II 57, 758–778. https://doi.org/10.1016/j.dsr2.2009.06.015.

Zapata, M., Jeffrey, S.W., Wright, S.W., Rodríguez, F., Garrido, J.L., Clementson, L., 2004. Photosynthetic pigments in 37 species (65 strains) of Haptophyta: implications for oceanography and chemotaxonomy. Mar. Ecol. Prog. Ser. 270, 83–102. https://doi.org/10.3354/meps270083.